Statistical Detection of Propagating Waves in a Polar Coronal Hole

G. R. Gupta[1,2], E. O'Shea[3], D. Banerjee[1], M. Popescu[3], and J. G. Doyle[3]

[1] Indian Institute of Astrophysics, Bangalore, India
[2] Indian Institute of Science, Bangalore, India
[3] Armagh Observatory, College Hill, Armagh, Northern Ireland

Summary. Waves are important in the heating of the solar corona and the acceleration of the solar wind. We have examined a long spectral time series sampling a southern coronal hole, observed on the February 25, 1997 with the SUMER spectrometer onboard SoHO. The observations used the spectra lines 765 Å, formed in the transition region, and 770 Å, formed in the low corona. The spectra indicate the presence of compressional waves with periods of about 18 min, and also significant power at shorter periods. Using Fourier techniques, we measured the phase delays between the intensity as well as the velocity oscillations in the two lines, as a function of frequency. From these measurements we derive the travel time of the propagating oscillations and so the propagation speeds of the waves producing the oscillations. Sincee the measured propagation speeds are subsonic, we conclude that the observed waves are slow magneto-acoustic ones.

1 Introduction

Coronal holes are regions of cool and low density plasma that appear relatively dark at coronal temperatures. The predominantly unipolar magnetic field in coronal hole regions is thought to give rise to the fast solar wind. A number of studies, e.g., Ofman et al. (1997, 2000); Banerjee et al. (2001); Popescu et al. (2005) have measured oscillations in coronal holes in the polar off-limb regions of the Sun. All of these studies point to the presence of compressional waves, thought to be slow magnetoacoustic waves as found by Deforest & Gurman (1998); O'Shea et al. (2006, 2007). Recently, Gupta et al. (2009) have reported the detection of these waves in the disk part of the polar coronal hole (hereafter PCH). They also find a difference in nature of the compressional waves between bright (network) and dark (internetwork) regions in the PCH. In this contribution, we extend such analysis to another dataset. More detail is given in Gupta et al. (2009).

2 Observations and data analysis

The data used in this analysis were taken on February 25, 1997, during 00:00–13:59 UT with the $1 \times 300''$ slit of SUMER and an exposure time of 60 sec, in the 765 Å and 770 Å lines in a southern PCH. Details of the data reduction are given in Gupta et al. (2009).

The chromosphere and transition region show enhanced-intensity network boundaries and darker internetwork cells. Presumably, the magnetic field is predominantly concentrated at the network boundaries and, within coronal holes, the footpoints of coronal funnels emanate from these network boundaries. Since the observing duration of this dataset is very long, the locations of bright and dark pixels along the slit change with time. For this reason, we have analysed the whole dataset pixel by pixel and timeframe by timeframe.
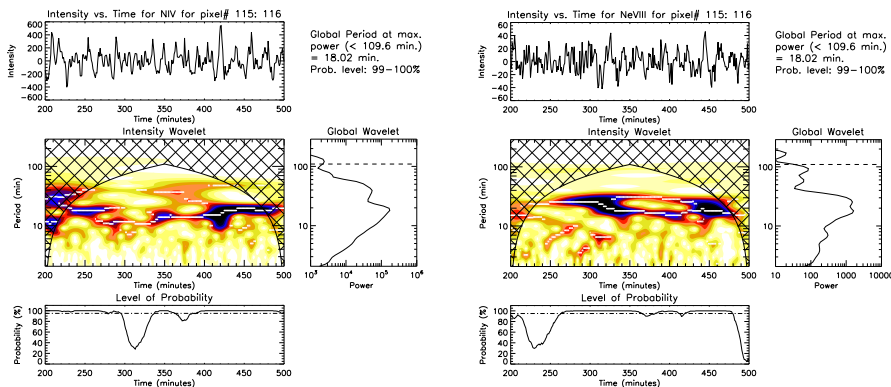

Fig. 1. Wavelet result for a bright location (pixels $115 - 116$, corresponding to $Y \approx -915''$) in the and intensities. In each set, the top panels show the relative (background trend removed) radiant flux, the central panels show the colour-inverted wavelet power spectrum, the bottom panels show the variation of the probability estimate associated with the maximum power in the wavelet power spectrum (marked with white lines), and the center-right panels show the global (averaged over time) wavelet power spectrum. Above the global wavelet the period, measured from the maximum power from the global wavelet and the probability estimate are specified.

For example, for one given moment we first determined the average intensity along the slit. All pixels having an intensity higher than 1.25 times this average intensity were chosen as bright pixels. If such pixels are bright for at least 60 min (or 60 timeframes), then these are considered to be a bright network location over that time interval. The bright pixel identification is done only for the low-temperature line; the network pixels obtained from it are assumed to be the same in the higher-temperature line.

3 Results and Discussions

Figure 1 shows a representative example of the oscillations measured in a bright region of the PCH. We use wavelet analysis to provide information on the temporal signal variation (Torrence & Compo 1998). Further details on this wavelet analysis are found in Gupta et al. (2009); O'Shea et al. (2001) and references therein. Figure 1 shows oscillations of about 18 min periodicity in both lines at the same location. This suggests that these two layers are linked by a propagating wave passing from one layer to the other. To test this hypothesis and to ascertain the nature of the propagating waves, we measured phase delays in intensity and in Dopplershift between the two lines at each of the measurable pixels along the slit for a full frequency range, following the method of Athay & White (1979), O'Shea et al. (2006), and Gupta et al. (2009) which deliver the phase delay, $\Delta\phi = 2\pi f T$ where f is the frequency and T the time delay in seconds. From this defintion, we expect that the phase difference varies linearly with f and will change by $360°$ over frequency intervals of $\Delta f = 1/T$, producing parallel lines in plots of $\Delta\phi$ versus f at fixed frequency intervals ($\Delta f = 1/T$), corresponding to a fixed time delay T.
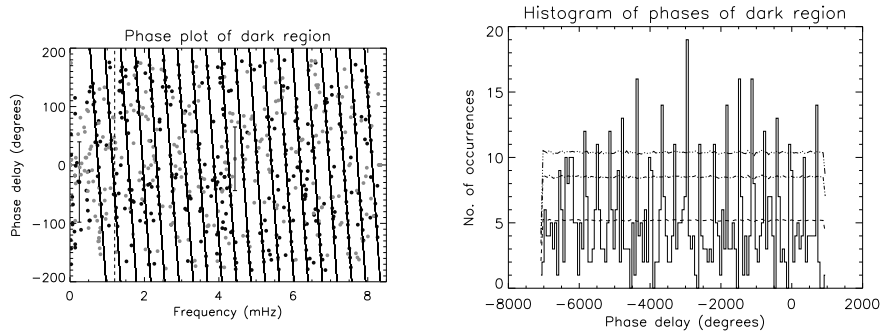

Fig. 2. Left-hand panel: Phase delays measured between oscillations in the spectroscopic line pair at dark locations. The phases from brightness oscillations are shown as grey dots, those from Doppler velocities as black dots. Overplotted are parallel lines, corresponding to fixed time delays. The vertical dashed line at 1.2 mHz indicates that phase values below this frequency may be affected by solar rotation. Representative errors on the phase measurements are indicated by error bars. Right panel: Histogram showing the distribution of the phase delay measurements as a function of frequency for the dark locations. The horizontal dotted, dot-dashed and long dashed lines show the 68.3% (1σ), 90% (1.64σ) and 95% (2σ) confidence levels, evaluated from Monte-Carlo simulations with 5000 permutations.

The method to identify the parallel lines in the phase plot (left-hand panel of Fig. 2) and their spacing and significance in the histogram (right-hand panel) is discussed in more detail in Gupta et al. (2009). In the bright location, we did not have good enough statistics to come to a reliable conclusion.

In the dark locations of the PCH (left-hand panel of Fig. 2), we measured a time delay of -2607 ± 491.2 s between the two lines, indicating upwardly propagating waves. Notice the many closely spaced, steeply sloped, parallel phase lines that correspond to this long time delay. In the right-hand panel of Fig. 2 these parallel phase lines correspond to significant peaks above 95% significance in the histogram. These peaks are equally spaced at the phase difference of 360°that would be expected for unimpeded propagating waves.

The measured time delays from this PCH may be used to estimate propagation speeds of the waves assumed to be causing the oscillations. In order to calculate the propagation speeds, one needs information on the formation height difference of the two lines. A value of 4095 km has been calculated using the limb brightening technique as described in O'Shea et al. (2006); Gupta et al. (2009). Using this height difference and the measured time delay, we find a speed of -1.6 ± 0.3 km s^{-1} for the dark region, which is smaller than the sound speed at that height. Hence, the identified waves can be identified as slow magneto-acoustic waves. These waves are rather slow and may not carry enough energy flux for the acceleration of the solar wind.

References

Athay, R. G. White, O. R. 1979, ApJ, 229, 1147

Banerjee, D., O'Shea, E., Doyle, J. G., Goossens, M. 2001, A&A, 380, L39

Deforest, C. E. Gurman, J. B. 1998, ApJ, 501, L217

Gupta, G. R., O'Shea, E., Banerjee, D., Popescu, M., Doyle, J. G. 2009, A&A, 493, 251

Ofman, L., Romoli, M., Poletto, G., Noci, G., Kohl, J. L. 1997, ApJ, 491, L111

Ofman, L., Romoli, M., Poletto, G., Noci, G., Kohl, J. L. 2000, ApJ, 529, 592

O'Shea, E., Banerjee, D., Doyle, J. G. 2006, A&A, 452, 1059

O'Shea, E., Banerjee, D., Doyle, J. G. 2007, A&A, 463, 713

O'Shea, E., Banerjee, D., Doyle, J. G., Fleck, B., Murtagh, F. 2001, A&A, 368, 1095

Popescu, M. D., Banerjee, D., O'Shea, E., Doyle, J. G., Xia, L. D. 2005, A&A, 442, 1087

Torrence, C. Compo, G. P. 1998, Bull. American Meteo. Soc., 79, 61